XLIII CILAMCE
21-25, November, 2022
FOZ DO IGUAÇU - PR - BRAZIL

Topology Optimization of Periodic Materials employing the Finite-Volume Theory

Arnaldo S. Júnior[1], Márcio A. A. Cavalcante[2]

[1] *Center of Technology, Federal University of Alagoas*
Av. Lourival Melo Mota, Tabuleiro do Martins, 57072-900, Maceió/AL, Brazil
arnaldo@ctec.ufal.br
[2] *Campus of Engineering and Agricultural Science, Federal University of Alagoas*
BR 104, Km 85, 57100-000, Rio Largo/AL, Brazil
marcio.cavalcante@ceca.ufal.br

Abstract. This paper presents a computational tool for designing composite materials with periodic microstructures for optimal effective elastic properties. The effective elastic properties of the periodic porous material are evaluated through a combination of the homogenization method and finite-volume theory analysis. The finite-volume theory results are employed in the topology optimization procedure, combining this technique with the dual optimization algorithm of convex programming. In this approach, to find the optimal microstructural topology for the periodic unit cell, specific linear combinations of the components of the effective elastic tensor are considered to obtain extreme elastic properties, such as the maximum shear or bulk modulus under a prescribed volume constraint. Some numerical examples involving materials with periodic porous microstructures are analyzed, and the results demonstrate the finite-volume theory formulation's performance for the optimal design of composite porous materials.

Keywords: Topology Optimization, Finite-Volume Theory, Homogenization, Material Design.

1 Introduction

Composite materials have gotten the interest of many researchers and found important applications in the more diverse modern industrial sectors because such materials, in general, present behavior quite different in comparison with the traditional homogeneous materials (Santos Júnior et al. [1]). Materials with porous microstructures correspond to a particular class of composite materials and are widely found in nature, such as honeycomb architecture, bone, and bamboo. The objective of the material design is to create a new microstructure that produces similar behavior to those natural materials.

Topology optimization (Bendøe and Kikuchi [2]) has grown as an interesting technique for designing microstructural topologies. Several studies have been developed to provide an efficient material layout accounting for the required performance and employing less material. In that regard, Wang et al. [3] provide a systematic and comprehensive review of educational articles and codes on structural and multidisciplinary optimization.

Initially presented by Bansal and Pindera [4], the finite-volume theory emerged as a powerful alternative to the established finite element method for analyzing structures and materials. According to Cavalcante et al. [5], this technique employs the volume average of the many fields that define the material's behavior and apply boundary and continuity conditions between adjacent subvolumes in an average sense. In the context of designing optimal structures, this theory was first employed by Araujo [6] and Araujo et al. [7, 8].

This work presents a computational tool based on finite-volume theory for designing periodic porous materials with extreme elastic properties. To verify the performance of this approach, some examples of periodic porous materials were analyzed and the results are discussed.

2 Finite-volume theory for periodic materials

The finite-volume theory version presented here corresponds to a zeroth-order formulation for rectangular analysis domain discretized in rectangular subvolumes based on an elastic mechanical stress analysis (Cavalcante and Pindera [9], Cavalcante et al. [10]). In this approach, the displacement field is approximated by the second-order Legendre polynomial expressed as a function of the local coordinates inside each subvolume, the boundary and continuity conditions are imposed in a surface-averaged sense, and the equilibrium equations are satisfied at the subvolume level.

Following Drago and Pindera [11], we consider periodic materials characterized by the basic building block called a repeating unit cell (RUC) which is replicated to generate the periodically repeating material microstructure, see Fig. 1. Hence, the response of the periodic material is characterized by the response of a single unit cell subjected to periodic boundary conditions. Such problems are typically treated using the asymptotic homogenization theory (Bensoussan et al. [12]). In its simplest form, the displacement field representation in the *qth* subdomain in terms of two-scale expansion in global and local coordinates (x_1, x_2) and (y_1, y_2), respectively, involving macroscopic and microstructure-induced fluctuating components are expressed by,

$$u_i^{(q)}(\boldsymbol{x},\boldsymbol{y}) = \bar{\varepsilon}_{ij}x_j + \tilde{u}_i^{(q)}(\boldsymbol{y}),\ \ (i = 1, 2), \tag{1}$$

where $\tilde{u}_i^{(q)}$ denote fluctuating displacement components induced by the heterogeneous microstructure and $\bar{\varepsilon}_{ij}$ are the specified macroscopic or average strains applied to the entire material.

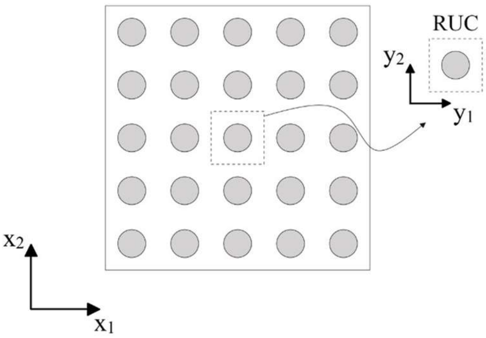

Figure 1. Periodic microstructure characterized by an RUC

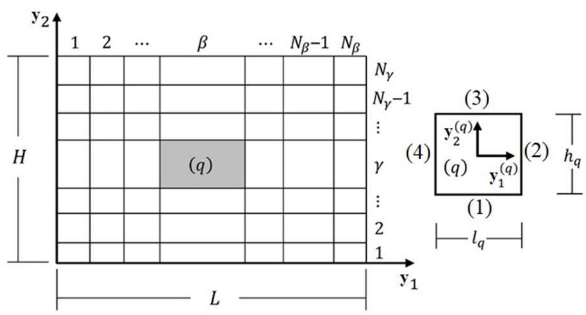

Figure 2. Discretized analysis domain and local coordinate system of a generic subvolume q

The rectangular domain in the y_1 - y_2 plane occupies the region $0 \le y_1 \le L$ and $0 \le y_2 \le H$, and is discretized into N_β horizontal subvolumes and N_γ vertical subvolumes denoted by pairs (β, γ), see Fig. 2. The subvolume dimensions are l_q and h_q for (β = 1,…, N_β and γ = 1,…, N_γ) along the y_1 and y_2 axes, respectively. Each subvolume may contain different elastic material characterized by constant moduli. In cartesian zeroth-order formulation, the components of the displacements field in the local coordinates system are approximated by the second-order polynomial (Cavalcante et al. [10]),

$$\tilde{u}_i^{(q)} = W_{i(00)}^{(q)} + y_1^{(q)}W_{i(10)}^{(q)} + y_2^{(q)}W_{i(01)}^{(q)} + \frac{1}{2}\left[3\left(y_1^{(q)}\right)^2 - \frac{l_q^2}{4}\right]W_{i(20)}^{(q)} + \frac{1}{2}\left[3\left(y_2^{(q)}\right)^2 - \frac{h_q^2}{4}\right]W_{i(02)}^{(q)}, \tag{2}$$

where $i = 1, 2$ and $W_{i(mn)}^{(q)}$ are unknown coefficients. These coefficients are expressed as a function of the surface-averaged fluctuating displacements as follows,

$$\begin{aligned}\hat{u}_i^{(q,p=1,3)} &= \frac{1}{l_q}\int_{-\frac{l_q}{2}}^{\frac{l_q}{2}} \tilde{u}_i^{(q)}\left(y_1, \mp\frac{h_q}{2}\right)dy_1 = W_{i(00)}^{(q)} \mp \frac{h_q}{2}W_{i(01)}^{(q)} + \frac{h_q^2}{4}W_{i(02)}^{(q)},\\ \hat{u}_i^{(q,p=2,4)} &= \frac{1}{h_q}\int_{-\frac{h_q}{2}}^{\frac{h_q}{2}} \tilde{u}_i^{(q)}\left(\pm\frac{l_q}{2}, y_2\right)dy_2 = W_{i(00)}^{(q)} \pm \frac{l_q}{2}W_{i(10)}^{(q)} + \frac{l_q^2}{4}W_{i(20)}^{(q)},\end{aligned} \tag{3}$$

where $\hat{u}_i^{(q,p)}$ corresponds to the surface-averaged fluctuating displacements on the face p of qth subvolume. The surface-averaged fluctuating displacements are then related to the surface-averaged tractions upon use of Cauchy's relations $t_i^{(q,p)} = \sigma_{ji}^{(q,p)}n_j^{(q,p)}$, the constitutive equations $\sigma_{ji} = C_{ijkl}\varepsilon_{kl}$, the kinematic relations between displacements and strains and the following definitions,

$$\hat{t}_i^{(q,p=1,3)} = \frac{1}{l_q}\int_{-\frac{l_q}{2}}^{\frac{l_q}{2}} t_i^{(q,p)}\left(y_1, \mp\frac{h_q}{2}\right)dy_1, \quad \hat{t}_i^{(q,p=2,4)} = \frac{1}{h_q}\int_{-\frac{h_q}{2}}^{\frac{h_q}{2}} t_i^{(q,p)}\left(\pm\frac{l_q}{2}, y_2\right)dy_2. \tag{4}$$

Employing the equilibrium equation at level of the *qth* subvolume,

$$\int_S \hat{\boldsymbol{t}}^{(q)} dS = \sum_{p=1}^{4}\int_{l_p} \hat{t}_i^{(q,p)} dl_p = \sum_{p=1}^{4} l_p \hat{t}_i^{(q,p)} = \mathbf{0}, \tag{5}$$

where $\hat{\boldsymbol{t}}^{(q)} = \left[\hat{t}_i^{(q,1)}\ \hat{t}_i^{(q,2)}\ \hat{t}_i^{(q,3)}\ \hat{t}_i^{(q,4)}\right]^T$. In linear elastic analysis, this leads to the local stiffness matrix for each *qth* subvolume,

$$\hat{\boldsymbol{t}}^{(q)} = \boldsymbol{H}^{(q)}\bar{\boldsymbol{\varepsilon}} + \boldsymbol{K}^{(q)}\hat{\boldsymbol{u}}^{(q)}, \tag{6}$$

where $\hat{\boldsymbol{u}}^{(q)} = \left[\hat{u}_i^{(q,1)}\ \hat{u}_i^{(q,2)}\ \hat{u}_i^{(q,3)}\ \hat{u}_i^{(q,4)}\right]^T$. The matrix $\boldsymbol{H}^{(q)}$ contains positive and negative elements of the stiffness matrix $\boldsymbol{C}^{(q)}$ whose sign depends on the direction of the unit normal vector associated with the given subvolume face, $\bar{\boldsymbol{\varepsilon}}$ is the macroscopic strain and $\boldsymbol{K}^{(q)}$ **i**s the local stiffness matrix.

According to Cavalcante et al. [10], imposition of traction and displacement continuity between adjacent subvolumes in a surface-average sense, together with periodic boundary conditions, produces the global system of equations for the unknown fluctuating surface-averaged interfacial displacements, symbolically expressed in the form,

$$\boldsymbol{K}\hat{\boldsymbol{u}} = \boldsymbol{\mathcal{H}}\bar{\boldsymbol{\varepsilon}}, \tag{7}$$

where $\hat{\boldsymbol{u}}$ is the global surface-averaged fluctuating displacements, $\boldsymbol{K}$ is the global stiffness matrix and $\boldsymbol{\mathcal{H}}$ corresponds to the matrix comprised of the differences in the material stiffness matrices of adjacent subvolumes.

3 Homogenization of periodic materials and sensitivity analysis

The effective elastic properties of periodic composite material can be evaluated by asymptotic homogenization theory (Bensoussan et al. [12). This theory corresponds to a solid mathematical formulation and provides rigorous convergence estimates of the displacements field. In its simplest form, the effective stiffness tensor is given by volume average over the base cell Ω as follows,

$$C_{ijkl}^H = \frac{1}{|\Omega|}\int_\Omega C_{ijpq}\left(\bar{\varepsilon}_{pq}^{(kl)} - \tilde{\varepsilon}_{pq}^{(kl)}\right)d\Omega, \tag{8}$$

where $|\Omega|$ denotes the area, for plane analysis, and $\tilde{\varepsilon}_{pq}^{(kl)}$ corresponds to periodic or fluctuating strain solution of,

$$\int_\Omega C_{ijpq}\varepsilon_{ij}(\upsilon)\tilde{\varepsilon}_{pq}^{(kl)} d\Omega = \int_\Omega C_{ijpq}\varepsilon_{ij}(\upsilon)\bar{\varepsilon}_{pq}^{(kl)} d\Omega, \tag{9}$$

where $\upsilon \in H_{per}^1(\Omega)$ which is Ω-periodic admissible arbitrary displacements field and $\bar{\varepsilon}_{pq}^{(kl)}$ the macroscopic or average strains applied to the entire material. In 2D analysis, $\bar{\varepsilon}_{pq}^{(kl)}$ corresponds to three linearly independent unit test strains field. Note that eq. (9) corresponds to the weak form of the standard elasticity equation applied to periodic boundary conditions. Employing the concept of element mutual energies (Sigmund [13], Xia and Breitkopf [14]), eq. (8) can be rewritten in equivalent form,

$$C_{ijkl}^H = \frac{1}{|\Omega|}\int_\Omega C_{pqrs}\varepsilon_{pq}^{A(ij)}\varepsilon_{rs}^{A(kl)} d\Omega. \tag{10}$$

where $\varepsilon_{pq}^{A(kl)}$ corresponds to superimposed strain field $\left(\bar{\varepsilon}_{pq}^{(kl)} - \tilde{\varepsilon}_{pq}^{(kl)}\right)$ in eq. (8). In the finite element analysis, the RUC is discretized into N_e elements and eq. (10) is approximated by,

$$C_{ijkl}^H = \frac{1}{|\Omega|}\sum_{e=1}^{N_e}\left(\boldsymbol{u}_e^{(ij)}\right)^T \boldsymbol{K}_e \boldsymbol{u}_e^{(kl)}, \tag{11}$$

where $\boldsymbol{u}_e^{(kl)}$ represents the local displacement field for each isolate test strain case $\bar{\boldsymbol{\varepsilon}}^{(kl)}$, and $\boldsymbol{K}_e$ the element stiffness matrix.

In this work, the finite-volume theory applied to the linear elastic analysis of periodic composite materials was constructed based on asymptotic homogenization theory for computing the displacement field on the RUC. In this context, the correspondent effective tensor (in matrix form) evaluated in terms of element mutual energies, similar to the finite element method analysis, can be assessed as follows,

$$C_{ijkl}^{H} = \frac{1}{|\Omega|}\sum_{q=1}^{N_q}\left(\boldsymbol{u}^{(q)}\Big|^{(ij)}\right)^T \boldsymbol{K}^{(q)}\boldsymbol{u}^{(q)}\Big|^{(kl)}, \tag{12}$$

where $\boldsymbol{u}^{(q)}\Big|^{(.)}$ denotes the subvolume surface-average displacement vector for each isolate test strain case $\bar{\boldsymbol{\varepsilon}}^{(.)}$.

The local material can be treated as isotropic for deriving the sensitivities in terms of the penalized elastic properties. In this sense, we employ the scheme proposed by Stolpe and Svanberg [15], known as the Rational Approximation of Material Properties (RAMP), to evaluate Young's modulus in terms of the density (ρ_q) at the level of the subvolume (q) as follows,

$$E^{(q)} = E_{min} + \frac{\rho_q}{1+p(1-\rho_q)}(E_0 - E_{min}),\ \rho_q \in [0,1]. \tag{13}$$

where p is the penalization factor, E_0 and E_{min} represent the Young's modulus of solid material and Young's modulus of the Ersatz material (to avoid singularity of stiffness matrix). This scheme presents a desirable feature, a nonzero sensitivity at zero density. According to Deaton and Grandhi [16], the RAMP method remedies some numerical difficulties due to very low-density problems. In this context, the sensitivities of C_{ijkl}^{H} is derived as,

$$\frac{\partial C_{ijkl}^{H}}{\partial \rho_q} = \frac{1}{|\Omega|}\frac{\partial E^{(q)}}{\partial \rho_q}\left(\boldsymbol{u}^{(q)}\Big|^{(ij)}\right)^T \boldsymbol{K}_0\boldsymbol{u}^{(q)}\Big|^{(kl)}. \tag{14}$$

where $\boldsymbol{K}_0$ denotes the subvolume stiffness matrix for a subvolume of solid material.

4 Topology optimization of material microstructure

Following Xia and Breitkopf [14], to obtain periodic porous material with extreme properties for specified boundary conditions and volume constraints, we define the mathematical formulation of the optimization problem as follows,

$$\begin{aligned} \underset{\rho}{Minimize}:&\quad \psi(C_{ijkl}^{H}(\boldsymbol{\rho})) \\ Subject\ to:&\quad \boldsymbol{K}\hat{\boldsymbol{u}}|^{(.)} = \boldsymbol{\mathcal{H}}|^{(.)}\bar{\boldsymbol{\varepsilon}} \\ &\quad \frac{1}{|\Omega|}\sum_{q=1}^{N_q} v_q\,\rho_q \le \vartheta \\ &\quad 0 \le \rho_q \le 1 \end{aligned} \tag{15}$$

where $\psi(C_{ijkl}^{H}(\boldsymbol{\rho}))$ corresponds to objective function, $\hat{\boldsymbol{u}}|^{(.)}$ and $\boldsymbol{\mathcal{H}}|^{(.)}$ the global surface-average fluctuating displacements vector and the matrix comprised of the differences in the material stiffness matrices of adjacent subvolumes for the isolate test strain (.), respectively, and ϑ denotes the volume fraction of solid material.

5 Numerical examples

To verify the performance of the finite-volume theory employed in the topology optimization design of porous materials with extreme elastic properties, some numerical examples are analyzed and the results consider three different initial design domains of porous material. The following examples adopted a solid material with Young's modulus $E = 1$, Poisson's ratio $v = 0.3$, a penalization factor $p = 5$, and the RUC discretized into 100 x 100 subvolumes for all analyses. The problem of eq. (15) is solved by the Optimality criteria method of the heuristic update scheme (Bendsøe and Sigmund [17]) with a damping factor set up to 0.5.

5.1 Maximizing the shear modulus

The objective function for maximization of the material shear modulus in plane stress analysis can be stated as follows,

$$\psi = -C_{1212}^{H}. \tag{16}$$

A comparison of final topologies of the RUC with maximum shear modulus and their correspondent effective elastic matrix for three different initial design domains is shown in Fig. 3 for no-filter scenario, considering the volume fraction of solid material $\vartheta = 0.5$. Different initial designs A and B, with the same porosities (12.64%), result in identical final topologies with similar shear modulus (0.1350). Figure 3 also shows the analysis results considering the initial design C with porosity equal to 25.68%, a combination of the initial designs A and B. This last analysis shows that the initial design domain affects the final topology because the algorithm is more likely to get trapped in a local minimum, as verified by Xia and Breitkopf [14]. Note that no checkboard pattern appears when the finite-volume theory is employed without a filtering technique. This important feature originates in the satisfaction of continuity conditions in a surface-averaged sense between adjacent subvolumes, which provides interfacial connections, differently from the displacement formulation of the finite element method, where the elements are connected through the nodes, Araujo [6] and Araujo et al. [7, 8]. Sometimes the array of 3x3 RUCs obtained from different initial design domains are shifted versions of the same topology, see red and blue square boxes in Fig. 3.

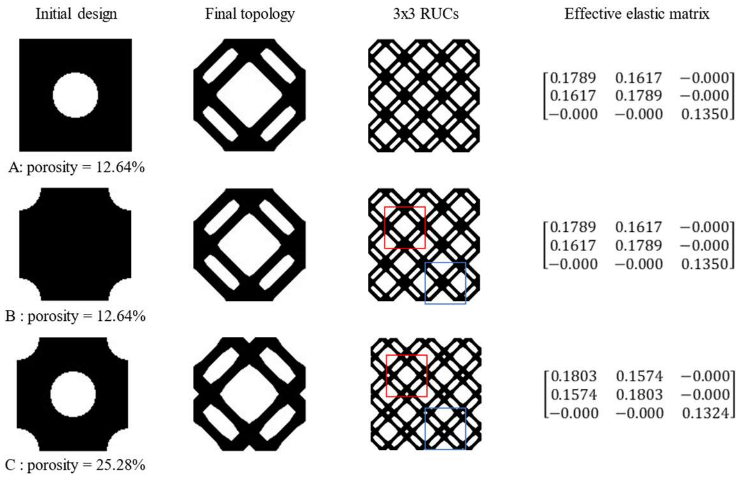

Figure 3. Microstructures of porous materials with maximum shear modulus and effective elastic matrices $\mathbf{C}^H$ – no-filter scenario

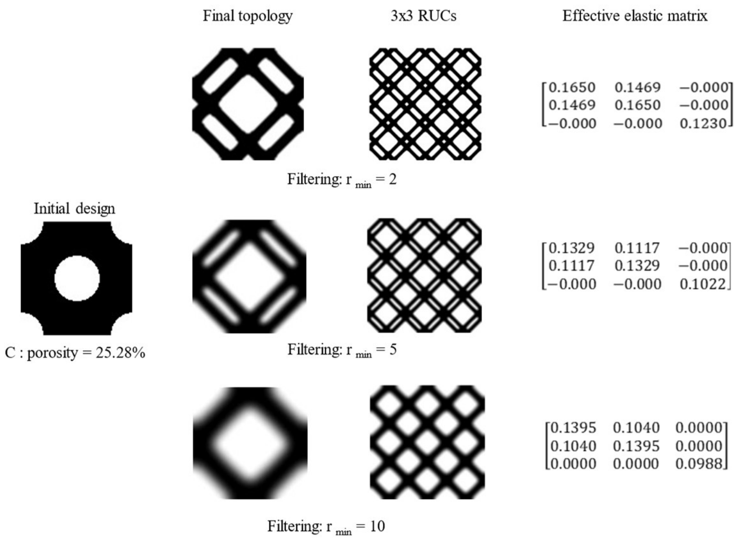

Figure 4. Final topologies of initial design domain C with maximum shear modulus and effective elastic matrices $\mathbf{C}^H$ in respect to density filter

To show the influence of filters on the final topology layout for maximization of material shear modulus, we consider the initial design C for the radius of filter r_{min} equal to 2, 5, and 10 times the dimension of the subvolume. The filtering technique employed here corresponds to the density filter presented by Andreassen [18]. Figure 4 illustrates that the choice of filter radius severely influences the final topology and the corresponding effective elastic properties, with a less complex topology for a higher filter radius, with the cost of a lower effective elastic property. The maximized effective shear modulus are 0.1230, 0.1022, and 0.0988 for the found optimum topologies, values corresponding to 93%, 77%, and 75% of the maximized effective shear modulus of 0.1324 obtained for a no-filter scenario, adopting the same initial design domain. Gray regions are also observed in the density filter scenario, especially for the largest filter radius.

5.2 Maximizing the bulk modulus

For maximizing bulk modulus of porous materials, the objective function is given with a linear combination of the components of effective elastic tensor. In plane stress analysis, the following expression can be adopted to maximize the material bulk modulus,

$$\psi = -\frac{1}{4}(C_{1111}^H + C_{1122}^H + C_{2211}^H + C_{2222}^H). \quad (17)$$

In Fig. 5, the initial designs A, B, and C were considered and the topology optimization results are produced when no filter and filtering schemes are employed to show the performance of the finite-volume theory in the design material with extreme bulk modulus. In this case, two different filter radii are adopted, and the volume fraction of solid material is $\vartheta = 0.5$. Once again, a checkboard pattern is not observed in the no filter scenario, with less influence of the initial design domain in the final design material in comparison with the density filter scenario. In other words, the no filter scenario is more stable considering the local minimum problem. Furthermore, gray regions are also observed in the density filter scenario, especially for the largest filter radius.

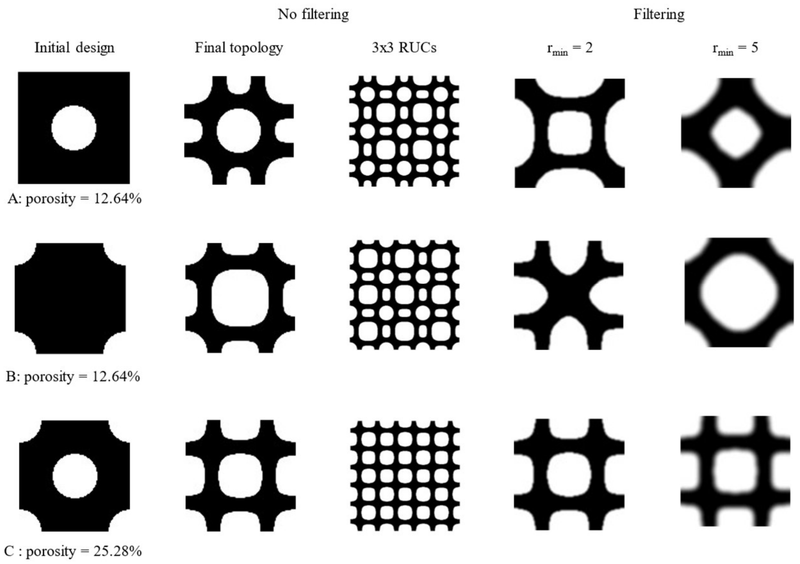

Figure 5. Comparison of microstructures of porous materials with maximum bulk modulus

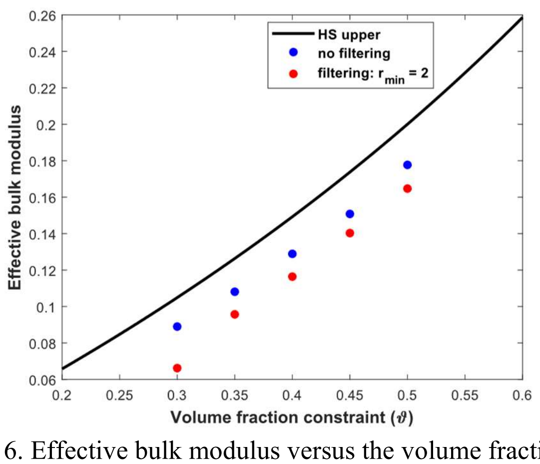

Figure 6. Effective bulk modulus versus the volume fraction constraints

Figure 6 shows the effective bulk modulus variation versus the solid material's volume fraction constraints (ϑ) for fixed filter radius r_{min} = 2 times the dimension of the subvolume. Topology optimization produces a final topology with the effective bulk modulus satisfying the Hashin-Shtrikman [19] upper bound. Furthermore, employing finite-volume theory without filtering techniques for material design results in higher effective elastic properties of the material.

6 Conclusions

In this investigation, the finite-volume theory was employed to analyze periodic porous medium in topology optimization for design materials. The results were shown for extreme material properties of shear and bulk modulus using the RAMP method for material penalization. Topologies obtained by finite-volume theory analysis when no filtering techniques are employed result in more complex designs without gray regions and no checkboard pattern, demonstrating efficiency for the analyzed examples. Besides, these topologies present higher values for the maximized effective elastic properties than those obtained in the density filter scenario. These preliminary results are encouraging but require more investigation.

Authorship statement. The authors hereby confirm that they are the sole liable persons responsible for the authorship of this work, and that all material that has been herein included as part of the present paper is either the property (and authorship) of the authors, or has the permission of the owners to be included here.

References

[1] A. Santos Júnior, S. P. C. Marques, M. A. A. Cavalcante, "A Study on Modeling Error Estimation in Elastic Structures of Heterogeneous Materials". Ibero-Latin American Congress on Computational Methods in Engineering (XXIX), 2008.
[2] M. P. Bendsøe, N. Kikuchi, "Generating optimal topologies in structural design using a homogenization method". *Computer Methods in Applied Mechanics and Engineering,* vol. 71, n. 2, pp. 197-224, 1988.
[3] C. Wang, Z. Zhao, M. Zhou, O. Sigmund, X. S. Zhang, "A comprehensive review of educational articles on structural and multidisciplinary optimization", *Structural and Multidisciplinary Optimization*, vol. 64, pp. 2827-2880, 2021.
[4] Y. Bansal, M.-J. Pindera, "Efficient reformulation of the thermoelastic higher-order theory for functionally graded materials". *Journal of Thermal Stress*. vol. 26, n. 11-12, pp. 1055-1092, 2003.
[5] M. A. A. Cavalcante, S. P. C. Marques, M. -J. Pindera, "Parametric formulation of the finite-volume theory for functionally graded materials – Part I: analysis". *Journal of Applied Mechanics,* vol. 74, n. 5, pp. 935-945, 2007.
[6] M. V. O. Araujo, "Teoria de Volumes Finitos Aplicada à Otimização Topológica de Estruturas Elásticas Contínuas". Msc. Thesis, Universidade Federal de Alagoas, 2018.
[7] M. V. O. Araujo, E. N. Lages, M. A. A. Cavalcante, "Checkerboard-free topology optimization for compliance minimization of continuum elastic structures based on the generalized finite-volume theory", *Latin American Journal of Solids and Structures*, vol. 17, n. 08, 2020.
[8] M. V. O. Araujo, E. N. Lages, M. A. A. Cavalcante, "Checkerboard free topology optimization for compliance minimization applying the finite-volume theory", *Mechanics Research Communications,* vol. 108, 2020.
[9] M. A. A. Cavalcante, M.-J. Pindera, "Generalized finite-volume theory for elastic stress analysis in solid mechanics –Part I: framework", *Journal of Applied Mechanics*, vol. 79, n. 5, pp. 051006-1, 2012.
[10] M. A. A. Cavalcante, M.-J. Pindera, H. Khatam, "Finite-volume micromechanics of periodic materials: past, present, and future", *Composites,* vol. 43, pp. 2521–2543, 2012.
[11] A. S. Drago, M.-J. Pindera, "Micro-macro mechanical analysis of heterogeneous materials: macroscopically homogeneous vs periodic microstructures". *Composites Science and Technology*, vol. 67, n. 6, pp. 1243-1263, 2007.
[12] A. Bensoussan, J-L. Lions, G. Papanicolaou, "Asymptotic analysis for periodic structures". North Holland, 1978.
[13] O. Sigmund, "Materials with prescribed constitutive parameters: an inverse homogenization problem". *International Journal of Solids and Structures*, vol. 31, n. 17, pp. 2313–2329, 1994.
[14] L. Xia and P. Breitkopf, P, "Design of materials using topology optimization and energy-based homogenization approach in Matlab", *Structural and Multidisciplinary Optimization*, vol. 1, 2015.
[15] M. Stolpe, K. Svanberg, "An alternative interpolation scheme for minimum compliance topology optimization". *Structural and Multidisciplinary Optimization*, vol. 22, n. 2, pp. 116–124, 2001.
[16] J. D. Deaton, R. V. Grandhi, "A survey of structural and multidisciplinary continuum topology optimization: post-2000". *Structural and Multidisciplinary Optimization*, vol. 49, n. 1, pp. 1–38, 2013.
[17] M. P. Bendsøe, O. Sigmund, "Topology optimization: theory, methods and applications". Springer, Berlin, 2003.
[18] E. Andreassen, A. Clausen, M. Schevenels, B. S. Lazarov, O. Sigmund, "Efficient topology optimization in MATLAB using 88 lines of code". *Structural and Multidisciplinary Optimization*, vol. 43, n. 1, pp. 1−16, 2011.
[19] Z. Hashin, S. Shtrikman, "A variational approach to the theory of the elastic behavior of multiphase materials". *Journal of Mechanics and Physics of Solids*, vol. 11, pp. 127–140, 1963.